Korean J. Chem. Eng., 35(12), 2348-2354 (2018)
DOI: 10.1007/s11814-018-0161-2

pISSN: 0256-1115
eISSN: 1975-7220

Techno-economic evaluation of the 2,3-butanediol dehydration process using a hydroxyapatite-alumina catalyst

Daesung Song*, Young-Gak Yoon, and Chul-Jin Lee**,†**

*Department of Civil, Safety & Environmental Engineering, Hankyong National University, 327 Jungang-ro, Anseong-si, Gyeonggi-do 17579, Korea
**School of Chemical Engineering and Materials Science, Chung-Ang University, 84 Heukseok-ro, Dongjak-gu, Seoul 06980, Korea
(*Received 1 July 2018 • accepted 8 October 2018*)

Abstract−We designed a conceptual model of the 2.3-BDO dehydration process using a hydroxyapatite-alumina catalyst and estimated its economic feasibility to predict the appropriate range of the purchase price of 2,3-BDO on commercial scale. The conceptual design and economic analysis can offer valuable information for the industrial application of 2,3-BDO because the most relevant studies have limitation in laboratory scale. Furthermore, the adequate range of 2,3-BDO price, in which the process has profitability, was investigated with the current market prices of 1,3-BD. The investigated price in terms of 2,3-BDO dehydration can pertain to estimation of the economic feasibility in 2,3-BDO production process.

Keywords: 2,3-Butanediol Dehydration, 1,3-Butadiene, Methyl Ethyl Ketone, Techno-economic Evaluation, Price of 2,3-Butanediol

INTRODUCTION

The production of chemicals from renewable sources has gained significant attention due to global environmental issues such as reduction of greenhouse gas emission. Industrial waste gas or lignocellulosic biomass as renewable feedstock could be converted into hydrocarbon fuels, furfural and 2,3-Butandiol (2,3-BDO). Carbon monoxide and carbon dioxide in industrial waste gas, which can bring environmental pollution, are changed to 2,3-BDO via microbial fermentation. Lignocellulosic biomass has significant potential to produce 2,3-BDO because it is abundant in agricultural and forestry residue [1,2].

The bio-derived 2,3-BDO is employed to develop sustainable chemical production as platform chemical having applicability to production of various derivatives such as 1,3-Butadiene (1,3-BD), Methyl ethyl ketone and so on [3-5]. Most of the research and development activities on bio-derived 2,3-BDO have been related to looking for microorganisms for its effective production and investigating appropriate catalyst to attain higher conversion on 2,3-BDO dehydration [6-11]. However, only a few discussions could be found that 2,3-BDO is capable of being used on commercial scale and have economic potential.

To obtain value-added chemical compounds such as 1,3-BD and MEK on industrial scale, the 2,3-BDO dehydration process was designed by Song et al. [12]. However, it investigates only technological and operating feasibility in terms of distillation. In addition, Apostolis et al. performed the modeling and economic evaluation in terms of 2,3-BDO production from glucose. From the 2,3-BDO price (approximately 2-5 $/kg), estimated by the authors, it is difficult to comprehend the overview at commercial scale because the authors excluded the point of 2,3-BDO utilization [13]. Penner et al. provided several simple models for MEK production, through 2,3-BDO produced from glucose, considering energy consumption [14].

This work investigated the 2,3-BDO dehydration process using $Ca_5(PO_4)_3(OH)$-Al_2O_3 as catalyst and investigated the economic value of 2,3-BDO at industrial scale. The proposed process can provide a detailed separation process for 1,3-BD and MEK. The profitability of the 2,3-BDO dehydration process was estimated. More importantly, the current price of 1,3-BD was applied at the economic evaluation and the feasible range of 2,3-BDO prices were predicted and presented.

MODELING AND SIMULATION

1. Thermodynamics

NRTL-RK is used as a thermodynamic model in the proposed process due to formation of water, ketone and alkene in 2,3-BDO dehydration. The main products including 1,3-BD and MEK are polar non-electrolytes, and the pressure in the overall process is not over 10 bars [15]. There are interaction parameters available in this liquid/liquid system, and NRTL binary parameters could be checked in the supporting materials (Table S1-S4).

2. Proposed Design

The process was modeled, using the Aspen Plus v8.4 software, to produce highly purified 1,3-BD and MEK via 2,3-BDO dehydration utilizing hydroxyapatite-alumina catalyst. The product specifications are that the product stream includes 1,3-BD and MEK above

†To whom correspondence should be addressed.
E-mail: cjlee@cau.ac.kr

Table 1. 2,3-BDO Dehydration reaction using hydroxyapatite-alumina catalyst

	Model Compound	Reaction
Main reaction	2,3-BDO→3B2OL	$C_4H_{10}O_2 \xrightarrow{-H_2O} C_4H_8O$
	3B2OL→1,3-BD	$C_4H_8O \xrightarrow{-H_2O} C_4H_6$
	2,3-BDO→MEK	$C_4H_{10}O_2 \xrightarrow{-H_2O} C_4H_8O$
Minor reaction	3B2OL→2Butene	$C_4H_8O \xrightarrow{+H_2-H_2O} C_4H_6$
	2,3-BDO→Acetoin	$C_4H_{10}O_2 \xrightarrow{-H_2} C_4H_8O_2$
	2,3-BDO→Oxirane	$C_4H_{10}O_2 \xrightarrow{-OH} C_4H_8O$
	2,3-BDO→Heavies	-

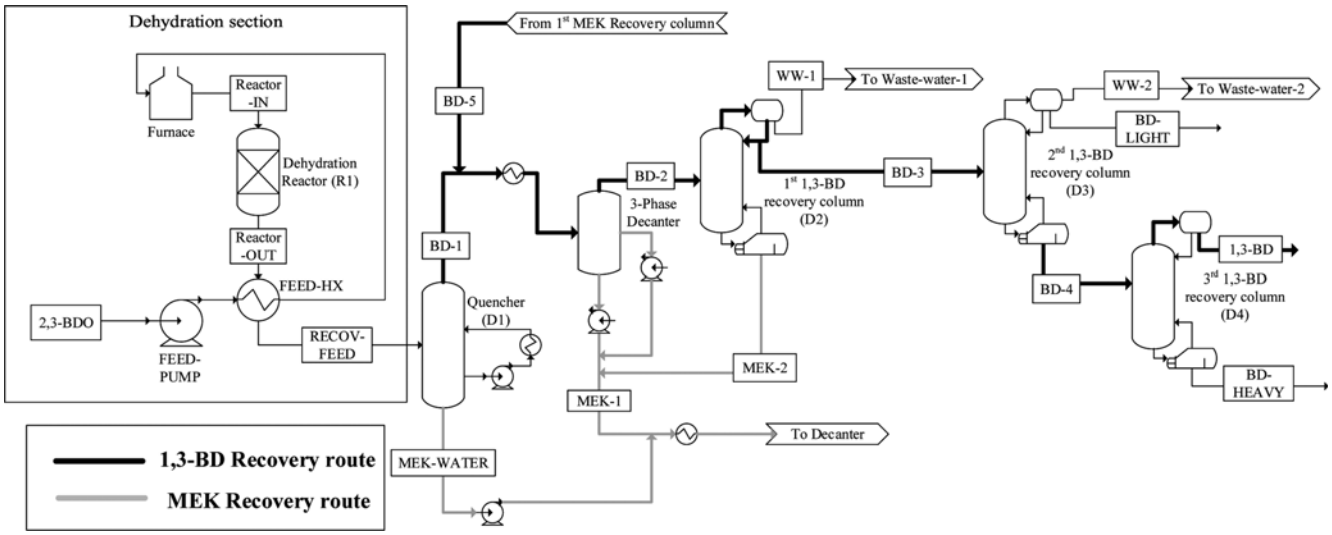

Fig. 1. Process flow diagram of dehydration section and 1,3-BD recovery section.

99.0 wt% and 99.5 wt%, respectively, and minor components are t-2butene (trans-2-Butene), c-2butene (cis-2-Butene), oxirane, water, acetoin, 3B2OL (3-Buten-2-ol), 2,3-BDO and heavies (3,5-Xylenol). Although there are several components heavier than 2,3-BDO in the proposed process, 3,5-Xylenol represents heavies to simplify the process simulation. That is because a negligible amount of the 'heavies' is produced, and thereby it has no impact on the separation process. The main and side chemical reactions are shown in Table 1 [3,16,17]. The proposed process is divided into three sections, 2,3-BDO dehydration, 1,3-BD recovery and MEK recovery. The information of the main streams and the specifications of each columns could be checked in the supporting material (Table S5-S8).

Table 2. Experimental conditions [16,17]

Contents	Description
Type of reactor	Stainless plug-flow reactor (inner diameter: 12 mm)
Catalyst	Hydroxyapatite-alumina catalyst (4.32 g)
Pressure	2 bar
Temperature	360 °C
Flow rate	3 ml/h, LHSV: 0.5 hr^{-1}
Sample analysis	Gas chromatography

Fig. 1 shows the process flow diagram (PFD), which is mainly composed of the dehydration and the 1,3-BD recovery sections. The dehydration section includes a furnace and a dehydration reactor.

Table 3. Product stream of the dehydration reactor (reactor-OUT)

Contents	Value
Temperature (°C)	360
Pressure (bar)	2.4
Vapor fraction	1
Mass flow (kg/h)	25,000
Mass fraction	
1,3-BD	0.364
MEK	0.248
H2O	0.317
Oxirane	0.033
Acetoin	0.005
3B2OL	0.018
2,3-BDO	0.008
1Butene	0.003
t-2Butene	0.002
c-2Butene	0.001
Heavies	0.001

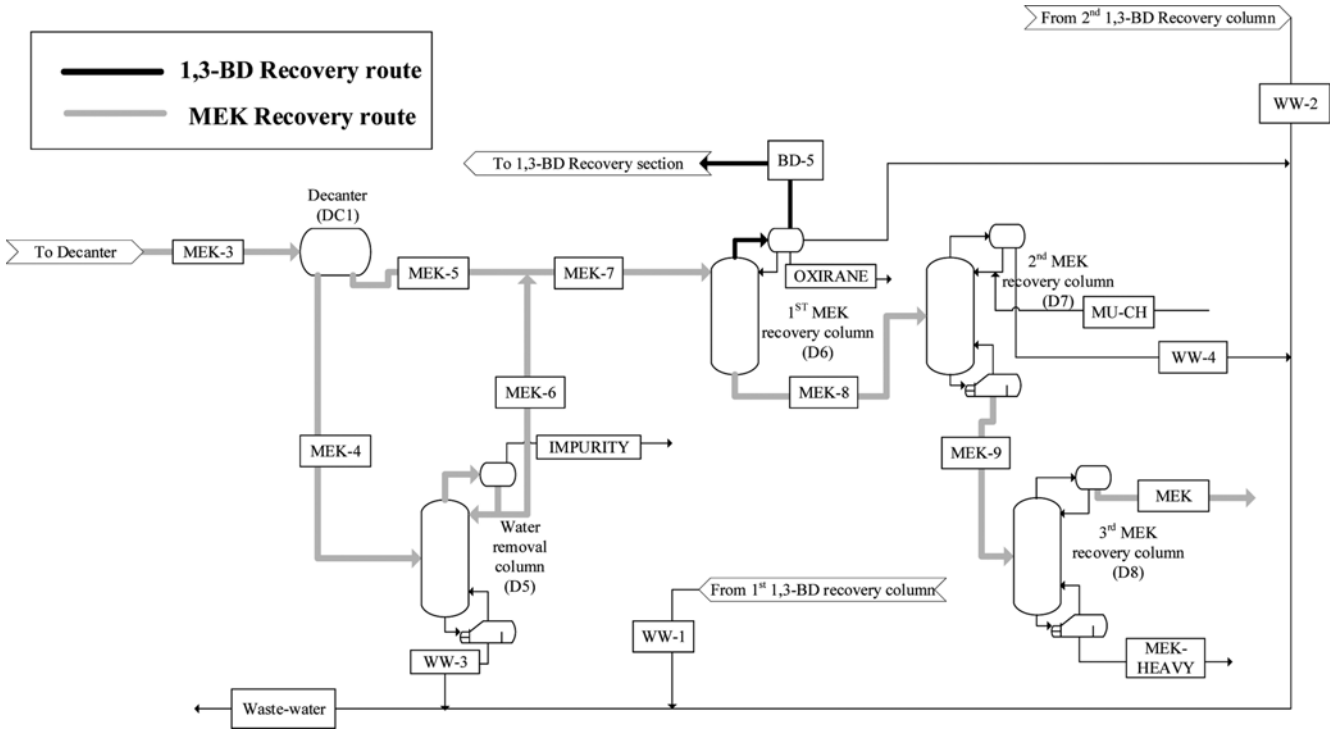

Fig. 2. Process flow diagram of MEK recovery section.

2,3-BDO (0.2 MMT/y) is fed to the dehydration reactor and it is simulated as an R-yield reactor, based on the experimental data in the laboratory. The experimental conditions are shown in Table 2. As for the experiment, 2,3-BDO (3 ml/h) is introduced into a stainless plug-flow reactor filled with 4.32 g of hydroxyapatite-alumina catalyst. The dehydration reactor is then operated at 2 bar and 360 °C. The remainder of the dehydration section represents the 1,3-BD recovery section, which is mentioned later in this section.

Table 3 shows the product stream information of the dehydration reactor, in which the mole fraction reflects the experimental data. The 2,3-BDO conversion of the dehydration reactor is 99.2%, and it is calculated using the following equation (Eq. (1)).

$$X_{2,3\text{-}BDO} = \frac{F_{2,3\text{-}BDO,\,in} - F_{2,3\text{-}BDO,\,out}}{F_{2,3\text{-}BDO,\,in}} \times 100 \quad (1)$$

where X is the conversion and F is the mass flow rate [kg/h].

The selectivity of 1,3-BD and MEK in the dehydration reactor is 36.8% and 25.1%, respectively, and it is calculated using the following equation (Eq. (2)).

$$S_{1,3\text{-}BD(MEK)} = \frac{F_{1,3\text{-}BD(MEK),\,out}}{F_{total} - F_{2,3\text{-}BDO,\,out}} \times 100 \quad (2)$$

where S is the selectivity and F is the mass flow rate [kg/h].

After the dehydration reaction, 1,3-BD is mainly discharged to the 1,3-BD recovery section through an overhead stream (BD-1) from a quencher (D1), in which the top temperature can be controlled by pumping around. MEK and water are transported to MEK recovery section through a bottom stream (MEK-WATER).

1,3-BD recovery section includes the 1st, 2nd, 3rd recovery columns (D2, D3, and D4) and 3-phase decanter, as shown in Fig. 1. The bold lines designate the main route of the 1,3-BD recovery. The overhead stream (BD-1) from the quencher (D1) is transported to the 1st 1,3-BD recovery column (D2) from which the remaining MEK and oxirane are removed and carried by a bottom stream (MEK-2). A portion of the overhead stream (BD-3) from the 1st 1,3-BD recovery column (D2) is transported to the 2nd 1,3-BD recovery column (D3) to separate the lighter component, 1butene (BD-LIGHT). Through the 3rd 1,3-BD recovery column (D4), heavier components such as t-2butene and c-2butene are separated from the main stream, which is transported from the bottom (BD-HEAVY) of the 2nd 1,3-BD recovery column (D3). In 1,3-BD recovery section, the operating pressure and temperature are decided to obtain the liquefied 1,3-BD product as a final product.

MEK recovery section consists mainly of 1st, 2nd, 3rd MEK recovery columns and Water Removal column (D6, D7, D8 and D5) in Fig. 2. The main stream to recover MEK is depicted using a gray line. The stream information and column specification of this part are also shown on the supporting materials (Table S5-S8). The stream from the bottom (MEK-WATER) of the quencher (D1) is directed to a decanter (3-phase decanter) with some parts separated from the 1,3-BD main stream (MEK-1) and the bottom stream (MEK-2) of the 1st 1,3-BD recovery column (D2 - Fig. 1). The aqueous phase and the organic phase from a decanter (DC1) shift to the water removal column (D5) and the 1st MEK recovery column (D6), respectively. In the water removal column (D5), water is removed and it goes through a bottom stream (WW-3), and part of an overhead stream (MEK-6) is transported to the 1st MEK recovery column (D6). Oxirane is mainly eliminated through an overhead stream of the 1st MEK recovery column (D6) and part of the overhead stream (BD-5) is combined with the overhead stream

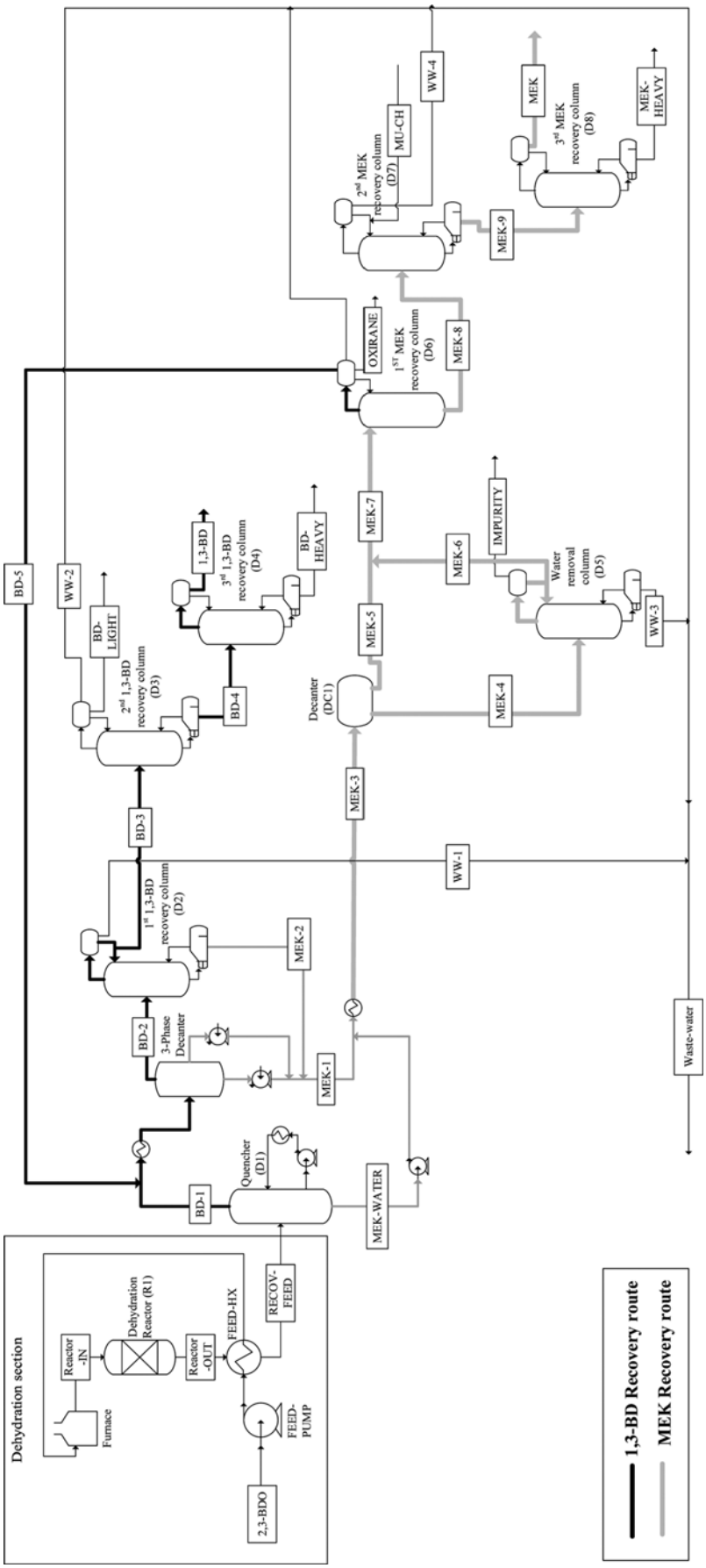

Fig. 3. 2,3-BDO dehydration process.

(BD-1) of the quencher (D1 - Fig. 1).

In the 2nd MEK recovery column (D7), among entrainers such as acetone, dimethylformamide and cyclohexane [18,19], cyclohexane (MU-CH) is used as the entrainer to break the azeotrope formed in the mixture of MEK and water because we investigated the purification of MEK through the comparison of experimental results and simulated data using cyclohexane [12]. MEK (MEK-9) separated from the azeotrope mixture is transported to the 3rd MEK recovery column (D8) through a bottom stream (MEK-9), and the water of an overhead stream (WW-4) is treated as waste water (Waste-water) with some water (WW-1, WW-2, WW-3, and WW-4) generated in the overall process. Heavier components such as 3B2OL, acetoin and oligomer are removed through a bottom stream (MEK-HEAVY) of the 3rd MEK recovery column (D8). The operating pressure of the 3rd MEK recovery column (D8) is below atmospheric pressure because the heavy compounds expected as naphtha and aromatic compounds can form oligomers giving rise to the operating problems. In addition, the entire process is represented in Fig. 3.

Table 4. Product streams of the proposed process (1,3BD and MEK)

Contents	1,3BD	MEK
Temperature (°C)	40.8	69
Pressure (bar)	4.4	2
Vapor fraction	0	0
Mass flow (kg/h)	8,318	6,116
Mass fraction		
1,3-BD	0.99	0
MEK	0	0.999
1Butene	0.003	0
t-2Butene	0.004	0
c-2Butene	0.002	0
3B2OL	0	0.001
Oxirane	0	0
H2O	0	0
Acetoin	0	0
2,3-BDO	0	0
Heavies	0	0

RESULTS AND DISCUSSION

1. Simulation Results

The 2,3-BDO capacity for the dehydration is 0.2 MMT/y (25,000 kg/h) in the proposed process. As shown in Table 4, two compounds are recovered having high purity (>99%), which is sufficient for the product specification (Table S9). The product flow rates of 1,3-BD and MEK are around 8,318 kg/h and 6,113 kg/h, respectively. The recovery rates of 1,3-BD and MEK are approximately 94% and 98.3%, respectively, as in the following equation (Eq. (3)).

$$R_{1,3\text{-}BD(MEK)} = \frac{1,3\text{-}BD(MEK)_{Product\ stream}[kg/h]}{1,3\text{-}BD(MEK)_{Reactor\ effluent}[kg/h]} \times 100 \quad (3)$$

where R is the recovery rate and 1,3-BD (MEK) is the mass flow rate of 1,3-BD (MEK) in the overall product stream.

2. Economic Evaluation

The total capital investment including the inside battery limits investment (ISBL) and the outside battery limits investment (OSBL) was used to evaluate the process, as shown in Table 5. ISBL includes the cost of the main process to manufacture the products and OSBL is the additional cost required for the process. The total capital investment was calculated using the factorial method. Essential features of ISBL, OSBL and factorial method have been described in the supporting materials (Table S10).

Several assumptions are applied in the economic analysis.

(1) The plant is located on the West Coast of the U.S.

(2) The feedstock is uniformly consumed at an amount of 25,000 kg/h.

(3) The plant operates during 8,000 hours annually.

(4) The plant is constructed mainly from a relatively expensive

Table 5. Factors and values of ISBL, OSBL and total fixed capital investment

Contents	Value [M$]
Purchased equipment	5.25
ISBL	19.6
OSBL	8.4
Total fixed capital investment	43.1

Table 6. Product cost summary

		Mass flow rate [kg/h]	Annual usage [kg/y]	Unit cost [$/kg]	Annual cost [M$]
Raw materials	2,3-BDO	25,000		0.8	160
	Catalyst		145,896	100	14.6
	Total				175
		Mass flow rate [kg/h]		Unit cost [$/kg]	Annual cost [M$]
Product	1,3-BD	8,318		1.62	107
	MEK	6,113		1.91	93.4
		Volumetric flow rate [m^3/h]		Unit cost [$/$m^3$]	Annual cost [M$]
	Fuel 1-3	1.20		549	5.29
	Total				205

material (SS304 or SS316), because 1,3-BD and MEK can affect the carbon steel.

(5) Two trains are installed, and each train involves two reactors. One train operates while catalyst in the other train is regenerated.

(6) The catalyst is used without a decrease in efficiency for three months. The annual amount of catalyst used is calculated in the experiment data (Section 2).

2-1. Payback Time

The payback time is the time required to recover an investment in terms of profits. It is useful to estimate the profitability of the project. The payback time is calculated using the following equation (Eq. (4)) [20].

$$\text{Payback Time [y]} = \frac{\text{Total fixed capital investment} + \text{Start up cost}}{\text{Profit (after taxes)} + \text{Depreciation}} \quad (4)$$

The start-up cost is typically computed to be 10% of the total fixed capital investment. The profit before taxes is shown in Table 6, and the taxes are measured using Turton's method [21]. The depreciation is 5% of the total fixed capital cost, the same as the running time of the plant.

2-2. Sensitivity Analysis

The price of 2,3-BDO is the decisive factor of profitability since it accounts for the largest portion of the total manufacturing cost of the proposed process, as illustrated in Fig. 4. However, the 2,3-BDO production limited in lab-scale makes it hard to provide the information of its industrial price. Therefore, we intend to carry out prediction of its price in this section. Given that the proposed process has economic feasibility, the price of 2,3-BDO could be investigated as a feedstock of the process. More importantly, because its profitability can be affected by severe fluctuation of the 1,3-BD price, the price of 2,3-BDO should be estimated essentially reflecting the variance of the market price of 1,3-BD, as represented in Table 7 [22,23].

A sensitivity analysis was carried out to estimate the prices of 2,3-BDO reflecting the fluctuation of the price of 1,3-BD. The price of MEK was assumed to be \$1.91/kg, which is the average value during seven years (2009-2015). Fig. 5 shows the range in which

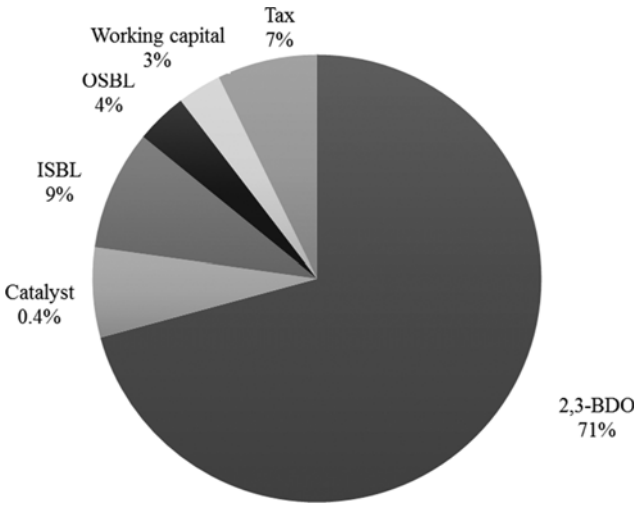

Fig. 4. Manufacturing cost diagram (1,3-BD: \$ 1.62/kg, MEK: \$ 1.91/kg and 2,3-BDO: \$ 0.8/kg).

Table 7. The prices of 1,3-BD and MEK (2009-2015)

Year	2009	2010	2011	2012	2013	2014	2015
1,3-BD [\$/kg]	2.06	4.20	6.39	4.59	2.93	2.82	1.76
MEK [\$/kg]	1.2	1.8	2.6	1.94	1.76	1.98	1.83

the process has economic feasibility, that is, the payback time is below 5 years [24]. In the feasible region the process has a stable feasibility regardless of the change in the prices of 1,3-BD and 2,3-BDO, given that the price of 1,3-BD maintained over \$ 2/kg in that period. In the other region profitability of the process can be seriously affected by the change of the 2,3-BDO price. When the price of 1,3-BD is \$ 1.62/kg, for instance, the payback time increases dramatically from 2.66 years to over 5 years increasing the price of 2,3-BDO from \$ 0.8/kg to \$ 0.9/kg. The example that 1,3-BD price changes is not particular. When the price of 2,3-BDO is \$ 0.8/kg, the payback time increases remarkably from 3.75 years to over 5 years dropping the price of 1,3-BD from \$ 1.5/kg to \$ 1.3/kg. There-

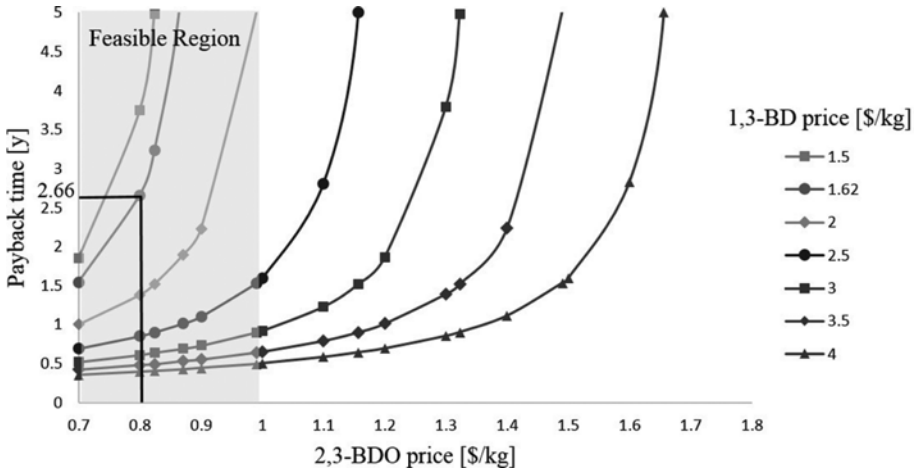

Fig. 5. Payback time on the prices of 2,3-BDO and 1,3-BD.

fore, the purchase price of 2,3-BDO should be evaluated conservatively because its price is a significant variable to ensure profitability of the process from the fluctuation of 1,3-BD price.

When the payback time is set up to 3 years to estimate the price of 2,3-BDO conservatively, as the current price of 1,3-BD varies from 2013 to 2015, the price of 2,3-BDO should be in the range ($ 0.991/kg-$ 1.3/kg) for this process to be economically feasible. As a result, the maximum purchase price (MPP) of 2,3-BDO is approximately $ 1.3/kg. However, it is eligible to have economic viability that the purchased price of 2,3-BDO maintains below around $ 0.991/kg. On such an occasion, 2,3-BDO can be assured of an alternative to produce 1,3-BD and MEK.

CONCLUSION

This research has conceptually designed a 2,3-BDO dehydration process to produce 1,3-BD and MEK utilizing hydroxyapatite alumina catalyst and evaluated its economic feasibility to predict the purchased price of 2,3-BDO. The proposed process is composed of the 2,3-BDO dehydration reactor according to the experiment data, the 1,3-BD recovery unit and the MEK recovery unit. The process has achieved approximately 94% and 98% recovery rates of 1,3-BD and MEK, respectively. With the consideration of the fluctuation of the current price of 1,3-BD, the economic assessment investigates the explicit variance of the payback time. The economically feasible price range of 2,3-BDO is estimated to be from $ 0.991/kg to $ 1.3/kg.

NOMENCLATURE

CH	: cyclohexane
c-2butene	: cis-2-butene
FCC	: fixed capital cost
ISBL	: inside battery limits investment
LHSV	: liquid hourly space velocity [hr^{-1}]
MEK	: methyl ethyl ketone
MPP	: maximum purchased price
NRTL	: non random two liquid model
NRTL-RK	: non random two liquid - redlich kwong model
OSBL	: outside battery limits investment
Oxirane	: 2,3-dimethyloxirane
PFD	: process flow diagram
t-2butene	: trans-2-butene
1,3-BD	: 1,3-butadiene
2,3-BDO	: 2,3-butanediol
3B2OL	: 3-buten-2-ol

ACKNOWLEDGEMENT

This research was supported by a grant (1615009755) from the Infrastructure and transportation technology promotion research program funded by the Ministry of Land, Infrastructure and Transport of the Korean government and by the Human Resources Development (No. 20184030202070) of the Korea Institute of Energy Technology Evaluation and Planning (KETEP) grant funded by the Korea government Ministry of Trade, Industry and Energy.

SUPPORTING INFORMATION

Additional information as noted in the text. This information is available via the Internet at http://www.springer.com/chemistry/journal/11814.

REFERENCES

1. X. Cui, X. Zhao and D. Liu, *Green. Chem.*, **20**, 2018 (2018).
2. M. Kopke, C. Mihalcea, F. Liew, J. H. Tizard, M. S. Ali, J. J. Conolly, B. Al-Sinawi and S. D. Simpson, *Appl. Environ. Microbiol.*, **77**, 5467 (2011).
3. D. Song, *Ind. Eng. Chem. Res.*, **55**, 11664 (2016).
4. D. Song, *Ind. Eng. Chem. Res.*, **56**, 11013 (2017).
5. D. Song, *Catalysts*, **8**, 72 (2018).
6. H. Duan, D. Sun, Y. Yamada and S. Sato, *Catal. Commun.*, **48**, 1 (2014).
7. H. Duan, Y. Yamada and S. Sato, *Appl. Catal A-Gen.*, **491**, 163 (2015).
8. S. V. Kannan and C. N. Pillai, *Indian J. Chem.*, **7**, 1164 (1969).
9. M. A. Nikitina, V. L. Sushkevich and I. I. Ivanova, *Petrol. Chem.*, **56**, 230 (2016).
10. H. Kim, H. Lee and D. S. Park, Korea Patent Patent 10-2014-0167303 (2014).
11. H. S. Kim, D. R. Park and H. W. Lee, Republic of Korea Patent US9511357 B2 (2015).
12. D. Song, Y.-G. Yoon and C.-J. Lee, *Chem. Eng. Res. Des.*, **123**, 268 (2017).
13. A. A. Koutinas, B. Yepez, N. Kopsahelis, D. M. G. Freire, A. M. de Castro, S. Papanikolaou and I. K. Kookos, *Bioresour. Technol.*, **204**, 55 (2016).
14. D. Penner, C. Redepenning, A. Mitsos and J. Viell, *Ind. Eng. Chem. Res.*, **56**, 3947 (2017).
15. E. C. Carlson, *Chem. Eng. Process.*, **October**, 35 (1996).
16. Y. Han and H. Kim, Republic of Korea Patent 10-1298672 (2013).
17. Y. Han, H. Kim, J. Hong and H. Jho, Korea Patent Patent 10-1287167 B1 (2013).
18. H. K. Kim, S. Y. Jung, C. Han, B. K. Na, Y. S. Chung and H. K. Song, *Korean. Chem. Eng. Res.*, **33**, 213 (1995).
19. H. M. L. a. H. L. Greene, *Adv. Chem.*, **115**, 148 (1974).
20. Y. Lim, C.-J. Lee, Y. S. Jeong, I. H. Song, C. J. Lee and C. Han, *Ind. Eng. Chem. Res.*, **51**, 4982 (2012).
21. R. Turton, R. C. Bailie, W. B. Whiting, J. A. Shaeiwitz and D. Bhattacharyya, Analysis, synthesis, and design of chemical processes, Pearson (2013).
22. E. Greiner, H. Janshekar, T. Kumamoto and E. Zhang, Chemical economics handbook: Methyl ethyl ketone (mek) (675.5000), IHS chemical (2015).
23. B. Hyde, R. Koster, W. Chen, A. Song, J. Maselli and S. Salamanca, Global c4 olefins & elastomers: Appendix, IHS chemical (2017).
24. J. M. Douglas, Conceptual design of chemical processes, Mc-Graw-Hill Chemical Engineering Series, New York (1988).

Supporting Information

Techno-economic evaluation of the 2,3-butanediol dehydration process using a hydroxyapatite-alumina catalyst

Daesung Song*, Young-Gak Yoon, and Chul-Jin Lee**,†**

*Department of Civil, Safety & Environmental Engineering, Hankyong National University,
327 Jungang-ro, Anseong-si, Gyeonggi-do 17579, Korea
**School of Chemical Engineering and Materials Science, Chung-Ang University,
84 Heukseok-ro, Dongjak-gu, Seoul 06980, Korea
(*Received 1 July 2018 • accepted 8 October 2018*)

Table S1. Binary parameters (1) (NRTL)

Component i	13BD	H2O	MEK	13BD	MEK	C-HEXANE	13BD	C-HEXANE	13BD	1BUTENE	1BUTENE	1BUTENE
Component j	H2O	23BDO	H2O	C-HEXANE	C-HEXANE	H2O	1BUTENE	1BUTENE	C2BUTENE	C2BUTENE	MEK	H2O
Temperature units	°C	°C	°C	°C	°C	°C	°C	°C	°C	°C	°C	°C
Source	APV86 LLE-ASPEN	APV86 VLE-RK	R-MEKH2O	NISTV86 NIST-RK	APV86 VLE-RK	APV86 LLE-ASPEN	APV86 VLE-RK	NISTV86 NIST-RK	APV86 VLE-RK	R-PCES	R-PCES	R-PCES
Property units												
AIJ	−1.6072	−2.4643	−1.04543	0	0	−10.4585	0	0.959752	0	0	0	0
AJI	−1.6062	6.5439	4.194684	0	0	13.1428	0	−0.71962	0	0	0	0
BIJ	2014.524	2482.862	588.2477	0	42.7828	4954.897	283.4563	0	12.7828	121.3348	299.3201	795.8132
BJI	2014.22	−2944.74	−459.012	0	371.2463	−1066.98	−223.035	0	−6.4297	−107.399	−32.2567	1629.561
CIJ	0.3	0.3	0.3	0	0.3	0.2	0.3	0.1	0.3	0.3	0.3	0.3
DIJ	0	0	0	0	0	0	0	0	0	0	0	0
EIJ	0	0	0	0	0	0	0	0	0	0	0	0
EJI	0	0	0	0	0	0	0	0	0	0	0	0
FIJ	0	0	0	0	0	0	0	0	0	0	0	0
FJI	0	0	0	0	0	0	0	0	0	0	0	0
TLOWER	7	58.4	−273.15	0	71.23	10	51.67	25	5	25	25	25
TUPPER	21	158.5	726.85	0	80.8	53	65.56	25	65	25	25	25

Table S2. Binary parameters (2) (NRTL)

Component i	1BUTENE	1BUTENE	13BD	13BD	13BD	C2BUTENE	C2BUTENE	C2BUTENE	C2BUTENE	C2BUTENE	MEK	MEK
Component j	23BDO	HEAVIES	MEK	23BDO	HEAVIES	MEK	C-HEXANE	H2O	23BDO	HEAVIES	23BDO	HEAVIES
Temperature units	°C	°C	°C	°C	°C	°C	°C	°C	°C	°C	°C	°C
Source	R-PCES	R-PCES	R-PCES	R-PCES	R-PCES	R-PCES	R-PCES	R-PCES	R-PCES	R-PCES	R-PCES	R-PCES
AIJ	0	0	0	0	0	0	0	0	0	0	0	0
AJI	0	0	0	0	0	0	0	0	0	0	0	0
BIJ	1342.937	450.4659	146.176	1093.292	324.5766	352.6867	126.9526	900.9591	1441.579	517.9601	563.836	−201.227
BJI	185.5662	−213.796	−0.06562	257.6139	−252.569	−39.2157	−94.9911	1599.288	168.5225	−210.014	−38.593	−341.48
CIJ	0.3	0.3	0.3	0.3	0.3	0.3	0.3	0.3	0.3	0.3	0.3	0.3
DIJ	0	0	0	0	0	0	0	0	0	0	0	0
EIJ	0	0	0	0	0	0	0	0	0	0	0	0
EJI	0	0	0	0	0	0	0	0	0	0	0	0
FIJ	0	0	0	0	0	0	0	0	0	0	0	0
FJI	0	0	0	0	0	0	0	0	0	0	0	0
TLOWER	25	25	25	25	25	25	25	25	25	25	25	25
TUPPER	25	25	25	25	25	25	25	25	25	25	25	25

Table S3. Binary parameters (3) (NRTL)

Component i	C-HEXANE	C-HEXANE	H2O	23BDO	13BD	C2BUTENE	1BUTENE	T2BUTENE	T2BUTENE	T2BUTENE	T2BUTENE	T2BUTENE
Component j	23BDO	HEAVIES	HEAVIES	HEAVIES	T2BUTENE	T2BUTENE	T2BUTENE	MEK	C-HEXANE	H2O	23BDO	HEAVIES
Temperature units	°C	°C	°C	°C	°C	°C	°C	°C	°C	°C	°C	°C
Source	R-PCES	R-PCES	R-PCES	R-PCES	APV86 VLE-RK	APV86 VLE-RK	R-PCES	R-PCES	R-PCES	R-PCES	R-PCES	R-PCES
AIJ	0	0	0	0	0	0	0	0	0	0	0	0
AJI	0	0	0	0	0	0	0	0	0	0	0	0
BIJ	1916.193	850.8401	1655.663	−773.007	53.6184	−0.1446	121.3348	352.6867	126.9526	900.9591	1441.579	517.9601
BJI	396.2759	−125.429	−109.014	211.7881	−42.1094	−0.957	−107.399	−39.2157	−94.9911	1599.288	168.5225	−210.014
CIJ	0.3	0.3	0.3	0.3	0.3	0.3	0.3	0.3	0.3	0.3	0.3	0.3
DIJ	0	0	0	0	0	0	0	0	0	0	0	0
EIJ	0	0	0	0	0	0	0	0	0	0	0	0
EJI	0	0	0	0	0	0	0	0	0	0	0	0
FIJ	0	0	0	0	0	0	0	0	0	0	0	0
FJI	0	0	0	0	0	0	0	0	0	0	0	0
TLOWER	25	25	25	25	5	5	25	25	25	25	25	25
TUPPER	25	25	25	25	65	85	25	25	25	25	25	25

Table S4. Binary parameters (4) (NRTL)

Component i	1BUTENE	13BD	T2BUTENE	C2BUTENE	OXIRANE	OXIRANE	OXIRANE	OXIRANE	OXIRANE
Component j	OXIRANE	OXIRANE	OXIRANE	OXIRANE	MEK	C-HEXANE	H2O	23BDO	HEAVIES
Temperature units	°C	°C	°C	°C	°C	°C	°C	°C	°C
Source	R-PCES	R-PCES	R-PCES	R-PCES	R-PCES	R-PCES	R-PCES	R-PCES	R-PCES
AIJ	0	0	0	0	0	0	0	0	0
AJI	0	0	0	0	0	0	0	0	0
BIJ	61.92255	−6.51317	87.77449	87.77449	186.3104	60.5337	384.6619	543.2968	−774.022
BJI	10.95519	70.97773	−3.57938	−3.57938	−94.0617	61.88439	1143.359	−164.901	1457.955
CIJ	0.3	0.3	0.3	0.3	0.3	0.3	0.3	0.3	0.3
DIJ	0	0	0	0	0	0	0	0	0
EIJ	0	0	0	0	0	0	0	0	0
EJI	0	0	0	0	0	0	0	0	0
FIJ	0	0	0	0	0	0	0	0	0
FJI	0	0	0	0	0	0	0	0	0
TLOWER	25	25	25	25	25	25	25	25	25
TUPPER	25	25	25	25	25	25	25	25	25

Table S5. Main stream information (1)

	2,3-BDO	Reactor-IN	Reactor-OUT	RECOV-FEED	BD-1	BD-2	BD-3	BD-4	BD-5	BD-LIGHT
Temperature, °C	25	360	360	180	68.5	90.2	37.9	44.4	39.8	99.1
Pressure, kg/sqcmg	0	1.5	1.4	0.9	0.8	4	4.2	3.958	1.1	-0.261
Vapor Frac	0	1	1	1	1	1	0	0	1	0
Mass flow, kg/hr	25000	25000	25000	25000	16810.22	10745.27	8898.145	8419.955	1228.723	191.336
Mass Frac										
1BUTENE	0	0	0.003	0.003	0.004	0.006	0.007	0.003	0.005	0
13BD	0	0	0.364	0.364	0.541	0.815	0.984	0.988	0.755	0
T2BUTENE	0	0	0.002	0.002	0.003	0.004	0.005	0.005	0.004	0
C2BUTENE	0	0	0.001	0.001	0.002	0.003	0.003	0.004	0.003	0
OXIRANE	0	0	0.033	0.033	0.048	0.044	0	0	0.222	0
MEK	0	0	0.248	0.248	0.347	0.114	0	0	0.001	0
C-HEXANE	0	0	0	0	0	0	0	0	0	0
3B2OL	0	0	0.018	0.018	0.002	0	0	0	0	0.579
H2O	0	0	0.317	0.317	0.052	0.014	0.001	0	0.011	0
ACETOIN	0	0	0.005	0.005	0	0	0	0	0	0.179
23BDO	1	1	0.008	0.008	0	0	0	0	0	0.068
HEAVIES	0	0	0.001	0.001	0	0	0	0	0	0.174

Table S6. Main stream information (2)

	BD-HEAVY	1,3BD	MEK-1	MEK-3	MEK-2	MEK-4	MEK-5	MEK-6	MEK-7
Temperature, °C	42.3	40.8	79.2	40	125.3	40	40	84.6	47.6
Pressure, kg/sqcmg	3.8	3.5	3.5	3.2	3.538	3.2	3.2	1.5	1.5
Vapor Frac	0	0	0	0	0	0	0	0	0
Mass flow, kg/hr	470.051	8317.929	17184.256	17184.26	1700.887	9139.326	8044.931	1461.852	9506.784
Mass Frac									
1BUTENE	0.067	0.003	0	0	0	0	0.001	0	0.001
13BD	0.931	0.99	0.074	0.074	0.001	0.006	0.152	0.035	0.134
T2BUTENE	0	0.004	0	0	0	0	0.001	0	0.001
C2BUTENE	0	0.002	0	0	0	0	0.001	0	0
OXIRANE	0	0	0.063	0.063	0.277	0.011	0.122	0.07	0.114
MEK	0	0	0.361	0.361	0.72	0.121	0.635	0.751	0.653
C-HEXANE	0	0	0	0	0	0	0	0	0
3B2OL	0	0	0.025	0.025	0.001	0.034	0.016	0	0.013
H2O	0.001	0	0.454	0.454	0	0.797	0.063	0.143	0.076
ACETOIN	0	0	0.007	0.007	0	0.009	0.004	0	0.004
23BDO	0	0	0.012	0.012	0	0.021	0.002	0	0.001
HEAVIES	0	0	0.002	0.002	0	0	0.004	0	0.004

Table S7. Main stream information (3)

	MEK-8	MEK-9	MEK	MU-CH	WW-1	WW-2	WW-3	WW-4	Waste-water	OXIRANE	IMPURITY
Temperature, °C	100.8	105.5	69	30	37.8	42.3	131.3	83	115.1	39.8	84.6
Pressure, kg/sqcmg	1.456	1.158	1	2	3.2	3.8	1.816	0.8	0.8	1.1	1.5
Vapor Frac	0	0	0	0	0	0	0	0	0.023	0	1
Mass flow, kg/hr	7049.338	6304.226	6112.89	0.429	146.244	8.139	7662.708	745.544	8590.736	1200.621	14.766
Mass Frac											
1BUTENE	0	0	0	0	0	0	0	0	0	0.002	0.002
13BD	0	0	0	0	0.008	0.001	0	0	0	0.287	0.368
T2BUTENE	0	0	0	0	0	0	0	0	0	0.002	0.002
C2BUTENE	0	0	0	0	0	0	0	0	0	0.001	0.001
OXIRANE	0	0	0	0	0	0	0	0	0	0.678	0.103
MEK	0.879	0.969	0.999	0	0	0	0	0.122	0.011	0.004	0.442
C-HEXANE	0	0	0	1	0	0	0	0	0	0	0
3B2OL	0.018	0.019	0.001	0	0	0	0.041	0.012	0.037	0	0
H2O	0.092	0	0	0	0.992	0.999	0.923	0.866	0.92	0.026	0.082
ACETOIN	0.005	0.005	0	0	0	0	0.011	0.001	0.01	0	0
23BDO	0.002	0.002	0	0	0	0	0.024	0	0.022	0	0
HEAVIES	0.005	0.005	0	0	0	0	0	0	0	0	0

Table S8. Column specification

Description	D1	D2	D3	D4	D5	D6	D7	D8
Number of stages, #	5	20	80	56	10	30	30	40
Pressure, kg/sqcmg	0.8	3.5	3.8	3.5	1.5	1.1	1.1	−0.3
Feed temperature, °C	180	90.2	38.0	44.4	40	47.6	101	106
Overhead temperature, °C	68.5	40.2	42.3	40.8	84.6	39.8	93.0	69.0
Bottom temperature, °C	97.2	125	44.4	41.9	131	100	105	99.1

Table S9. Product specification of 1,3-BD and MEK

Characteristic	Unit	Minimum	Maximum	Test Method
BD	wt%	99.0		ASTM D 2593
Peroxide	wt ppm		Max. 10	ASTM D 1022
Acetylenes	wt ppm		Max. 400	ASTM D 2593
Carbonyl compounds as acetaldehyde	wt ppm		Max. 100	ASTM D 4423
Butadiene dimer	wt%		Max. 0.2	ASTM D 2426
Non-volatile matter	wt%		Max. 0.1	ASTM D 1025
Total sulfur	wt ppm		Max 10	ASTM D 2784
MEK	wt%	99.5		GC
Water	wt%		0.1	ASTM D1364
Acidity as acetic acid	wt%		0.003	ASTM D1613
Non-volatile residue	mg/100 ml		2	ASTM D1353

Table S10. Result of economic assessment [1,2]

Contents		Factor	Value [M$]
ISBL	Purchased equipment, $C_{e,i,CS}$ (C_p^0)	1	5.25
	Equipment erection, f_{er}	0.3	1.58
	Instrumentation and controls, f_i	0.3	1.58
	Piping, f_p	0.8	4.2
	Electrical, f_{el}	0.2	1.05
	Structures and Buildings, f_s	0.2	1.05
	Civil, f_c	0.3	1.58
	Lagging and paint, f_l	0.1	0.53
	Total		19.6
OSBL		40% of ISBL	8.4
Design and engineering		30% of ISBL	5.89
Contingency		10% of ISBL	1.96
Fixed capital cost (FCC)			
Working capital		20% of FCC	7.17
Total fixed capital investment			43.1

The total capital investment including the inside battery limits investment (ISBL) and the outside battery limits investment (OSBL) is used to evaluate the process. The total capital investment is calculated using the factorial method. ISBL includes the cost of the main process to manufacture the products. It is a fixed investment without escalation for a plant. The items of the ISBL are mainly composed of the process equipment, building, piping, instrument and control, electrical system, lagging and painting, and civil. The purchased cost (C_p^0) is estimated using Turton's method (Eq. (S1)), and the other costs are assessed using Towler's method (Eq. (S2)), respectively [1].

$$\log_{10}C_p^0 = K_1 + K_2\log_{10}(A) + K_3(\log_{10}(A))^2 \quad (S1)$$

where A is the capacity or size parameter for the equipment. C_p^0 is the purchased cost, the data for K_1, K_2 and K_3 are given by Turton. This purchased cost is based on carbon steel as a material.

$$C = \sum_{i=1}^{i=M} C_{e,i,CS}((1+f_p)f_m + (f_{er}+f_{el}+f_i+f_c+f_s+f_l)) \quad (S2)$$

where $C_{e,i,CS}$ is the purchased cost of the equipment i in carbon

steel and is equal to C_p^0. The information for each factor is specified in Table S10. f_m means (purchased cost in exotic material)/ (purchased cost in carbon steel), and the value is 1.3 in this analysis.

OSBL includes the additional cost required for the main process. It includes the necessary and auxiliary costs to operate the plant. The items of the OSBL typically consist of a storage system, a steam generation unit, a cooling water system and a water treatment system. In this analysis, OSBL is calculated to be 40% of ISBL by factorial method [2]. In addition, the offsite costs, contingency, working capital, design and engineering are estimated in Table S10.

REFERENCES

1. R. Turton, R. C. Bailie, W. B. Whiting, J. A. Shaeiwitz and D. Bhattacharyya, Analysis, synthesis, and design of chemical processes, PEARSON (2013).
2. G. Towler and R. Sinnott, Chemical engineering design, Butterworth-Heinemann (2013).